

SIMULATIONS OF TENSILE FRACTURE IN CONCRETE

A. Vervuurt, M.R.A. Van Vliet, J.G.M. Van Mier and E. Schlangen.
Stevin Laboratory, Delft University of Technology
Delft, The Netherlands

Abstract

Fracture of heterogeneous materials like concrete, rock and ceramics is a complex process. Numerical continuum models have not lead to a unique solution for modelling concrete fracture at the macro-level. Especially localization from distributed microcracks to macro-cracking has proven to be very harsh. Simulating specimen behaviour at a lower scale (meso-level or microlevel) of the material seems to be more successful. A lattice type model has been proposed about five years ago at the Stevin Laboratory (Schlangen & Van Mier, 1992). The model simulates concrete cracking by removing a little piece of material (one lattice beam) from the finite element mesh. Every time a beam is removed, the maximum load which can be carried at that time is calculated from a linear elastic analysis. Through the years several lattice types have been applied to simulate concrete fracture. In this paper an overview is given of most of these lattices. A simulation of tensile fracture in a single edge notched (SEN) specimen, is used to compare the behaviour of the various lattice types. A remeshing procedure which has been developed recently will be discussed as well. Next to the application of the tensile test, a new splitting experiment and a shear test is simulated with this remeshing technique.

1 Introduction

Over half a century ago, Hrennikoff (1941) was one of the first to propose a truss model for simulating problems of elasticity. Because of limited calculation capacity however, Hrennikoff's framework method never left the shelves of academia. With the advanced computer techniques of the last years, lattice models have received new attention. Herrmann & Roux (1989) reintroduced a lattice model where a square grid of beams (Fig. 1a) was used to model fracture in disordered materials. A square lattice of beams leads to a Poisson's ratio equal to zero. Using a triangular lattice of trusses, the Poisson's ratio changes to 0.33. Both a square grid and a triangular grid seem not applicable for concrete, because of the mismatch in Poisson's ratio. When the truss model is changed to a triangular beam model (Fig. 1b and 1c), the Poisson's ratio can be changed by varying the cross sectional area of the beams. Heterogeneity of the lattice is already available when a random distribution is assigned to the length of the beams, as shown in Fig. 1c (Moukarzel & Herrmann, 1992). When a regular triangular lattice (Fig. 1b) is used, heterogeneity has to be implemented separately (Schlangen, 1993). Projecting the material structure which has to be simulated on top of the lattice, is a method which will be discussed in this paper.

Through the years several (triangular) lattice types have been applied for simulating cracking of concrete under mode I. Applications are for example given in Schlangen (1993), Schlangen (1995), Van Mier & Vervuurt (1994) and Vervuurt et al. (1994). In all lattice types presented in this paper, fracture is simulated by simply removing an element from the finite element mesh in each load step, which is assumed to be linear elastic. In spite of the local linear elasticity and purely brittle behaviour of the lattice elements, global softening of the material is obtained. The failure mechanism of crack face bridging in concrete (Van Mier, 1991) is simulated very realistically with the model, especially when the material structure is projected on top of the lattice.

In this paper examples will be given of an uniaxial tensile test simulated with different lattice types. Regular as well as random triangular lattices are utilized. For introducing the heterogeneity of concrete in the finite element

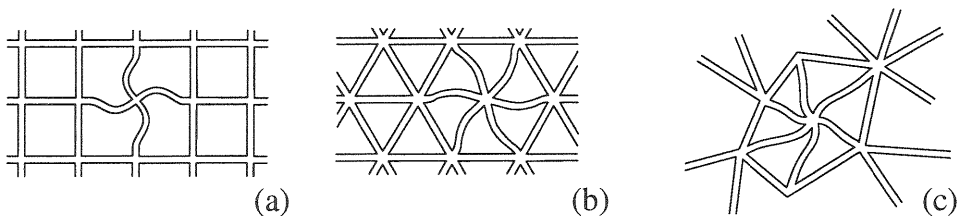


Fig. 1. Beam-lattice models. (a) regular square lattice, (b) regular triangular lattice and (c) random triangular lattice

model, several methods are given. In section 4 also some applications are given of specimens loaded under biaxial tension/shear after Noor-Mohamed (1992) and a splitting test which is presented in this proceedings (Vervuurt & Van Mier, 1995). Further simulations of the tensile/shear experiments have been carried out, and are presented in this proceedings by Schlangen (1995).

2 Lattice models including heterogeneity

2.1 Regular lattice

The regular triangular lattice as shown in Fig. 1b acts homogeneous if no heterogeneity is implemented separately. A rather simple way to achieve this is by assigning the beams with a random strength and stiffness. Looking at the structure of the material, it seems more realistic to use a (generated or scanned) grain structure as an overlay on top of the lattice. The strength and stiffness of each beam can be determined subsequently from the position of the beam in the grain structure (Fig. 2). In the figure, 'A' represents the aggregate phase, 'M' the matrix and 'B' the bond between matrix and aggregate. The regular lattice with a grain structure overlay applied in this paper, will be referred to as *TYPE A*. Table 1 at the end of section 2.2 shows an overview of all the lattice types used in this paper.

For the grain structure, circles are generated according to a Fuller curve discretization derived by Walraven (1980). The particles are placed randomly in a 2D box from which the required grain structure is selected. Two different methods for placing the particles in the box are applied. The first method is discussed in detail by Schlangen (1993), and consists of randomly placing the particles in the box. First the largest particles are placed, followed by the smaller particles. A random X- and Y-value is chosen for the center of the particle and a check is performed on earlier placed particles whether no overlaps appear. This procedure however, is very time consuming because a particle has to be replaced (and checked again) as soon as an overlap appears. Especially when a very dense aggregate structure is

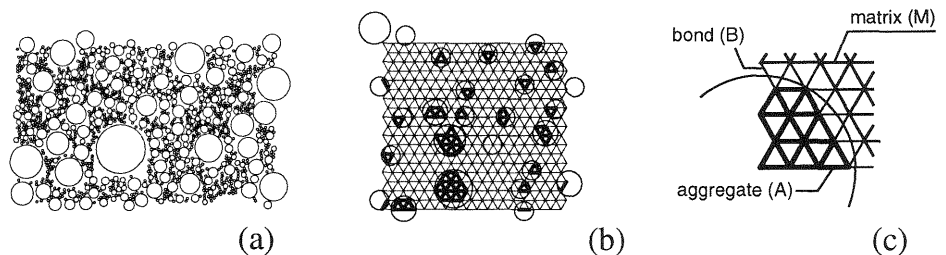


Fig. 2. Grain structure (a) projected on top of a regular triangular lattice (b) and (c) assigning properties to the beams in each phase

generated, this may lead to enormous computational efforts. Recently a new placing procedure has been developed which is much more efficient. Out of the generated particles, the particle which is to be dropped is selected at random. In stead of choosing both a random X- and Y-value, only X is chosen at random. The Y-coordinate is determined by dropping the particle from the top of the box. As soon as the particle touches one of the earlier dropped particles, the Y-coordinate is fixed. To make the particle structure more compact, this particle placement procedure can be repeated several times in order to determine the lowest particle position. Because the generated grain structure does not include all particles (the smallest have to be omitted) a minimum distance between two aggregates is prescribed. The distance between the two particle centers is calculated as $d_{min}=\gamma*(R_1+R_2)$, where R_1 and R_2 are the respective particle radii. The empirical factor γ is fixed as soon as the box is filled appropriately. Next to the minimum aggregate size, also the step size in the Fuller discretization influences this factor. The grain structure shown in Fig. 2a is a part of the structure used for the simulations presented in this paper, and contains particles between 0.25 and 8 mm, generated using a step size of 0.25 mm. Each particle was dropped 10 times from random positions on the top of the box. When a grain structure with less aggregates is used, the smaller particles can be omitted easily. For lattice *TYPE A* all aggregates smaller than 3.0 mm were excluded from the grain structure, because of the rather large length of the beams (5/3 mm) compared to the minimum aggregate size in the grain structure. The aggregate sizes used for the simulations presented here, are given in the overview at the end of section 3 (Table 2). It is mentioned that with the latter particle placement procedure, holes are formed under large particles, as can be seen in Fig. 2a. This phenomenon becomes stronger when the particle placement procedure is repeated less often.

2.2 Random lattices

Next to generating a grain structure for introducing heterogeneity in the finite element mesh, a disordered structure of the mesh can be used. A triangular lattice with a random length of the beams already exhibits a natural heterogeneity. In this paper two different types of random lattices are used. The first one has already been tested extensively in Schlangen (1993) and Vervuurt et al. (1994), and will only be pointed out briefly. The procedure for generating the mesh was developed earlier by Moukarzel & Herrmann (1992). Lattice *TYPE D* (Table 1) has a regular square grid as a basis (cell size $s=1.0$ mm, see Fig. 3a). In each cell of the grid a node is selected at random and next the lattice is defined by connecting always the three nodes which are closest to each other. Also a combination of lattice *TYPE A* and *TYPE D* can be used, i.e. a random lattice with particle overlay. This lattice is not applied in this paper but an example is given in Van Mier & Vervuurt (1995).

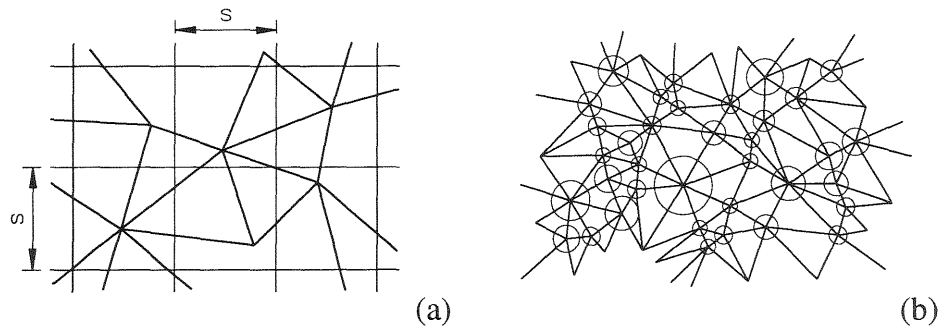


Fig. 3. Applied random lattices; (a) generation of a random lattice based on a regular square grid and (b) a random lattice structure based on the particle centers

A variant to the random lattice based on a regular square grid, is when the nodes are not fixed to any cell structure. A possible nodal structure for concrete is using the particle overlay as shown in section 2.1 (see Fig. 3b). The construction the lattice can proceed in a similar way as the random lattice based on a grid structure, i.e. connecting always the three nodes (particle centers) which are closest to each other. It may be obvious that the density of the mesh strongly depends on the minimum aggregate size in the particle structure. In this paper one particle structure is used from which two lattices were constructed. Lattice *TYPE B* (Table 1) was generated for particles between 0.50 and 8.0 mm. For the second "center particle lattice" (*TYPE C*), all particles smaller than 0.75 mm were excluded from the grain structure.

Finally a remeshing procedure is adapted for the random lattice based on a regular square grid (*TYPE E* in Table 1). The remeshing procedure is as follows. First of all, one fine and one coarse nodal structure is generated for the specimen to be simulated. Each nodal structure is based on the square grid shown in Fig. 3a. Subsequently the nodes from the fine structure ($s=1.0$ mm) are projected around the crack tip (or initially at the notch). The remainder of the specimen is overlaid with nodes from the coarse nodal structure ($s=5.0$ mm). Next the mesh is generated according to the procedure described above. As soon as the propagating crack reaches the coarse mesh

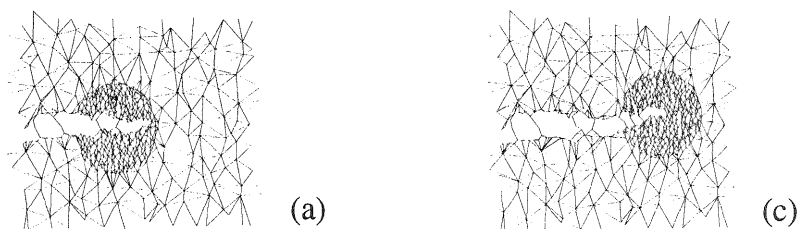


Fig. 4. Remeshing technique. Two stages of crack growth are shown

(Fig. 4a), remeshing is started. A new area is defined for the fine mesh and the former fine structure is replaced by the coarse mesh (Fig. 4b). Only nodes from the fine mesh along the crack are kept intact, which allows for crack face bridging outside the fine region. In the coarse mesh itself, no cracks are allowed to appear.

Table. 1: Overview of the lattice types used in this paper.

Lattice Type	Abbreviation
Regular lattice with grainstructure overlay	<i>TYPE A</i>
Random lattice based on a grainstructure	<i>TYPE B</i> <i>TYPE C</i>
Including particles between 0.50 and 8.0 mm	
Including particles between 0.75 and 8.0 mm	
Random Lattice based on a grid	<i>TYPE D</i> <i>TYPE E</i>
Based on a single grid	
Based on a double grid	

3 Parameter identification

For the lattice model, two types of parameters can be distinguished, i.e. properties regarding the linear elastic material behaviour and fracture parameters. The geometric properties of the beams (height h , thickness t as well as the Young's modulus E) are determined in a rather straightforward manner (Schlangen, 1993). The thickness of the beams is chosen equal to the thickness of the simulated specimen. The height h and the local E of the beams depends on the global Young's modulus and Poisson's ratio of the modelled material. After selecting a local E for the beams, h is fixed. When a grain structure is used as an overlay on top of the lattice (*TYPE A*)

Table. 2: Overview of parameters used in the various lattice types.

Lattice Type	Particles	E_A/E_B	E_M/E_B	f_{t_A}/f_{t_B}	f_{t_M}/f_{t_B}	Cell Size (mm)	Beam Height (mm)
<i>TYPE A</i>	3.0-8.0	70/25	25/25	8.0	4.0	5/3*	1.13
<i>TYPE B</i>	0.50-8.0	1.0		1.0		-	0.99
<i>TYPE C</i>	0.75-8.0	1.0		1.0		-	1.44
<i>TYPE D</i>	-	1.0		1.0		1.0	0.73
<i>TYPE E**</i>	-	1.0		1.0		1.0	0.73

* Beam length rather than cell size

** Indicated parameters refer to the fine lattice structure

different Young's moduli have to be assigned for each of the three phases, as mentioned in section 2.1 (Fig. 2c). The degree of heterogeneity of the material is determined by the two ratios of the three Young's moduli, E_A/E_B and E_M/E_B . Next to these ratios, heterogeneity is varied by changing the beam strength ratios f_{t_A}/f_{t_B} and f_{t_M}/f_{t_B} , where f_t is the stress at which a beam is assumed to fail. When no aggregate overlay is used (*TYPE B,C,D,E*) all ratios are equal to 1.0 and disorder depends only on the geometric irregularities of the mesh. It should be mentioned that we do not know the relation between the disorder in the random lattices and the heterogeneity of the material. Contrary to the previously mentioned parameters, the beam strength is a fracture parameter. The stresses in the beams are calculated as a combination of the normal force and the bending moments in a beam. Two additional parameters which are added to the fracture law will not be discussed here but the reader is referred to Schlangen (1993) and Vervuurt et al. (1994). An overview of the parameters for the lattice types presented in this paper is given in Table 2.

4 Applications

4.1 Uniaxial tension

The five different lattice types described in the first part of this paper have been used for simulating a uniaxial tensile test. The specimen with dimensions 100x200 mm (thickness 50 mm) is single edge notched at half height. The net area at the notch is 85x50 mm². The specimen is loaded by translating the (fixed) boundaries at the top and the bottom of the specimen parallel to each other. The crack opening plotted in the stress-crack opening diagrams (Fig. 5g) is the average of the deformations measured at the left and right side of the specimen. The measuring length was 35 mm. In the stress-crack opening diagrams, the stresses and deformations are normalized, using a factor β . It is mentioned that β depends on the lattice type and therefore differs for each simulation. Next to the stress-crack opening diagrams, crack patterns obtained with the corresponding lattice types are given (Fig. 5a-f). For lattice *TYPE E* two stages of crack growth are shown (Fig. 5e and 5f). The remaining lattice types are illustrated with one crack pattern only. Only the area where a lattice is used is shown. It can be seen that especially *TYPE A* shows quite realistic crack growth. Microcracks are initiated along the bond between matrix and aggregate. In a later stage microcracks join to localized macro cracks. The final crack patterns however are comparable for all lattices used, as are the computed stress-crack opening diagrams. A general conclusion which can be drawn is that more details in the crack pattern are obtained as soon as more detail is included in the finite element mesh. More details can be achieved by an aggregate overlay (*TYPE A*) or a smaller beam length. Moreover *TYPE E* seems extremely

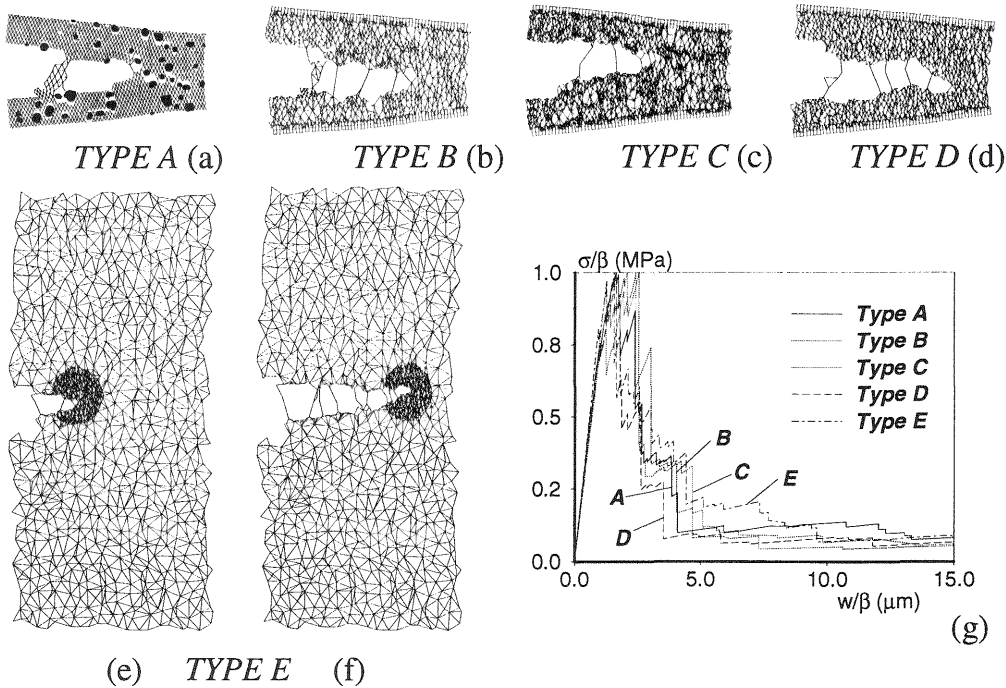


Fig. 5. Crack patterns (a-f) and dimensionless load-deformation curves (g) for the simulations

suitable for simulating specimens where the direction of crack growth is hard to predict. The amount of beam elements mostly depends on the area where a fine lattice is used. Curved crack growth for instance requires a rather large area modelled with a fine lattice of beams. In the following section two examples of curved crack growth are given.

4.2 Splitting and shear loaded specimens

In this final section two additional applications of lattice *TYPE E* are given. A new splitting type experiment as presented in this proceedings (Vervuurt & Van Mier, 1995) is simulated. The second application is the biaxial tensile/shear experiment after Nooru-Mohamed (1992). In the splitting experiment a horizontal load is applied to the steel loading platens at the top of the specimen (Fig. 6a). The specimen is supported at the bottom. The specimen in Fig. 6b is loaded by a horizontal translation of the upper loading platen. The lower loading platen is fixed in two directions while the upper one can move in the vertical direction. More details about loading and boundary conditions will not be discussed here. The reader is therefore referred to Vervuurt & Van Mier (1995) and Nooru-Mohamed (1992) for the splitting test and the tensile/shear experiment respectively.

The crack patterns shown in Fig. 6 are quite similar to the experimentally obtained results. The most significant gain in the remeshing technique is the

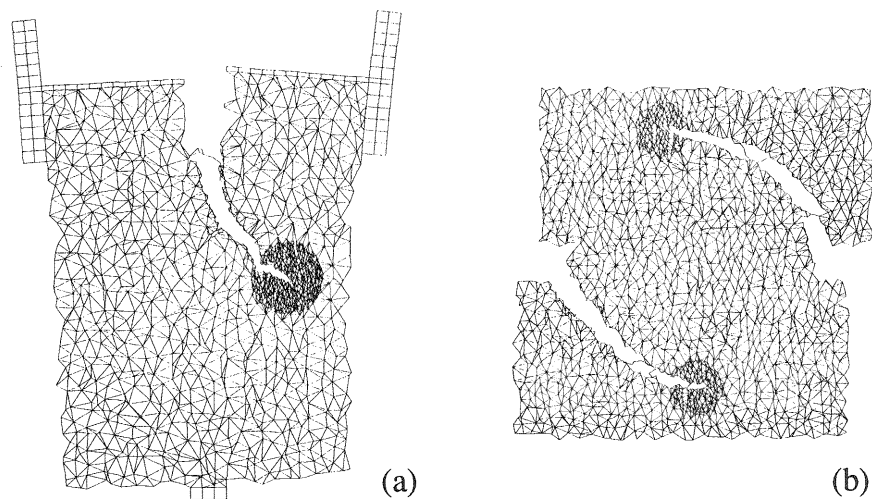


Fig. 6. Crack patterns for a simulation of (a) a splitting test after Vervuurt & Van Mier (1995) and (b) a shear loaded test (Nooru-Mohamed, 1992)

reduction of the amount of beams necessary for modelling the specimen, and thus the computational capacity needed. Only the place where localized crack growth starts, has to be known in advance. For example for the splitting test (Fig. 6a) an enormous reduction of beam elements is obtained, because crack growth can proceed either to the left or right side of the specimen. Next to this advantage also a disadvantage should be mentioned. Because no distributed (non-localized) microcracks are allowed to grow outside the fine region around the crack tip (except for the bridges) the lattice is applicable only for rather brittle materials. Compared to the SEN tensile test performed with lattice *TYPE A* (Fig. 5a) too little microcrack growth is allowed in the specimens modelled with lattice *TYPE E* (Fig. 5e, 5f and Fig. 5). It therefore is rather debatable whether this technique is useful for simulating fracture in concrete. Then, especially when large aggregates are included, large crack face bridges and a wide range of microcracks are observed (Van Mier, 1991).

5 Conclusions

A lattice model is described for simulating cracking in concrete specimens. Heterogeneity is implemented in several ways, and five different lattice types have been applied in the simulation of a SEN tensile test. It is shown that the final crack patterns and the stress-crack opening diagrams are quite similar for all lattices. If more detail is included in the mesh, more detail in the crack patterns is obtained. More detail can be included by refining the mesh or by projecting the material structure on top of the lattice. The latter method prevails. A new remeshing technique is presented in this paper as well.

The remeshing technique seems extremely effective when the crack path is hard to predict. For highly heterogeneous materials however, the remeshing procedure seems less suitable.

References

- Herrmann, H.J., Hansen, A. and Roux, S. (1989) Fracture of disordered, elastic lattices in two dimensions. **Phys. Rev. B**, 39(1), 637-648.
- Hrennikoff, A. (1941) Solutions of problems of elasticity by the framework method. **J. of Applied Mech.**, A169-A175.
- Moukarzel, C. and Herrmann, H.J. (1992) A vectorizable random lattice, **Preprint HLRZ 1/92**, HLRZ KFA Jülich.
- Nooru-Mohamed (1992) Mixed Mode Fracture of Concrete: an Experimental Approach. PhD-Thesis, Delft University of Technology.
- Schlangen, E. (1993) Experimental and Numerical Analysis of Fracture Processes in Concrete. PhD-Thesis, Delft University of Technology.
- Schlangen, E (1995) Computational aspects of fracture simulations with lattice models, in **this proceedings**.
- Schlangen & Van Mier (1992) Experimental and numerical analysis of micromechanisms of fracture of cementbased composites. **Cem. & Concr. Composites** (ed. V.C. Li), 14(2), 105-118.
- Van Mier, J.G.M. (1991) Mode I fracture of concrete: discontinuous crack growth and crack interface grain bridging. **Cem. & Concr. Res.**, 21, 1-15.
- Van Mier, J.G.M. and Vervuurt, A. (1995) Lattice model for analysing steel-concrete interface behaviour, in **Mechanics of geomaterial interfaces** (eds. A.P.S. Selvadurai & M.J. Boulon), Elseviers Science B.V., Amsterdam, 201-225.
- Vervuurt, A. and Van Mier, J.G.M. (1995) Interface fracture in cement-based materials, in **this proceedings**.
- Vervuurt, A., Van Mier, J.G.M. and Schlangen, E. (1994) Analyses of anchor pull-out in concrete. **Mat. & Struct.**, 27, 251-259.
- Walraven, J.C. (1980) Aggregate Interlock: a Theoretical and Experimental Analysis. PhD-Thesis, Delft University of Technology.